

## COUPLED STRESS AND ENERGY ANALYSIS OF CRACK ONSET IN TEXTILE COMPOSITES AT THE MESOSCOPIC SCALE

M. Hirsekorn<sup>1</sup>, Aurélien Doitrand<sup>1</sup>, Christian Fagiano<sup>1</sup>, and Vincent Chiaruttini<sup>1</sup>

<sup>1</sup>Onera - The French Aerospace Lab, 29 Avenue de la Division Leclerc, F-92322 Châtillon, France  
Email: martin.hirsekorn@onera.fr, Web Page: <http://www.onera.fr>

**Keywords:** textile composites, FE modeling, damage, coupled criterion, experimental observation

### Abstract

A coupled stress and energy criterion is used to analyze crack initiation at the mesoscopic scale in a four-layer plain weave glass-epoxy composite. The choice of possible crack configurations is restricted based upon optical microscope observations of damage mechanisms on a specimen edge during tensile testing. It is found that transverse yarn cracking accompanied by yarn-yarn decohesions around the crack tips is the first damage that occurs in the composite. For the stress condition in the yarns, a criterion developed for modeling failure of unidirectional plies in a laminate is applied. For the energy condition, the difference between the potential energies of an undamaged and a cracked unit cell is calculated, using identical mesh topologies. The energy criterion is found to be dominant in the studied case. It leads to an estimation of the crack initiation strain much closer to experimental observations by acoustic emission than the stress criterion alone and allows to determine crack length and orientation at damage onset. The coupled criterion leads to the conclusion that the yarn-yarn decohesions are a direct consequence of the transverse yarn cracks, and its length can be determined through the energy criterion.

### 1. Introduction

The prediction of damage onset by means of numerical modeling is one of the great challenges for the industries using composite parts with textile reinforcements. The mechanical performance of textile composites depends on the reinforcement architecture, which is defined at the so-called mesoscopic scale (at which consolidated yarns are considered as homogeneous material embedded in a matrix). It has been shown in several studies that the local strain distribution and hence damage onset depends not only on the weaving pattern, but also on the yarn waviness [1-2] and the relative shifts and nesting between the layers of the reinforcing fabric [3-4]. It is therefore important to take into account the layer shifts and the effects of fabric compaction during the manufacturing process in order to obtain a reinforcement geometry for damage modeling that is close to those of real composite specimens [5-6].

In most published works on damage modeling in textile composites, a stress based criterion is used to predict damage onset from the stress fields obtained from a Finite Element (FE) model of a representative unit cell (RUC) of the composite [1-2, 7-9]. It is often used together with continuum damage mechanics approaches [1-2, 8] to model the effect of damage via a progressive reduction of the material properties. However, these methods lead to mesh depending results and erroneous prediction of the damage propagation directions [8, 10] if no suitable regularization technique is used [11-12]. The latter leads to a non-local damage zone and hence avoids mesh dependence. In this case, the FE mesh must be very fine compared to the geometric features of the RUC in order to model the experimentally observed localized cracks, which results in high computational costs.

An alternative approach, which is closer to the experimental observations at the mesoscopic scale, is discrete damage modeling [6, 13-14] by inserting cracks directly into the FE mesh. A stress based criterion seems to be appropriate to predict the crack location [6] but not its length. Furthermore, it is only a necessary condition for crack initiation but not a sufficient one, as enough energy must be provided to overcome the material toughness in order to open a crack [15-16]. The consequence of this coupled stress and energy criterion is that at weak stress singularities or at non-singular stress concentrations (as occur in the undamaged zones of textile composites), cracks of finite size are generated instantaneously [16]. The crack configuration is given by the state that fulfills both the energy and the stress criterion over the whole crack surface for a minimum global strain. The coupled criterion has been successfully used at the macroscopic scale to model the strength of an open hole composite plate [17], at the mesoscopic scale to predict delamination of angle-ply laminates [18], and at the microscopic scale to analyze fiber-matrix decohesion [19]. In this contribution, we present its application to the prediction of crack onset at the mesoscopic scale in a multi-layer woven composite. In Section 2, the experimentally observed crack configurations are presented with the aim of restricting the possible crack configurations studied numerically. Section 3 summarizes the procedure of crack insertion into a meso-scale textile composite RUC. In Section 4, the coupled criterion is defined and its application to the case of textile composites is explained. Section 5 presents the results of this study.

## 2. Experimental observations

The composite under investigation consists of four layers of an E-glass fiber plain weave fabric embedded in an Araldite LY564 epoxy matrix. Before resin injection, the fabric is compacted in a steel mold by tightening the screws that keep the mold closed. Rectangular specimens were tested under monotonic tensile load using acoustic emission (AE) sensors to detect damage onset and optical microscope observations on the specimen edge to determine the crack configurations.

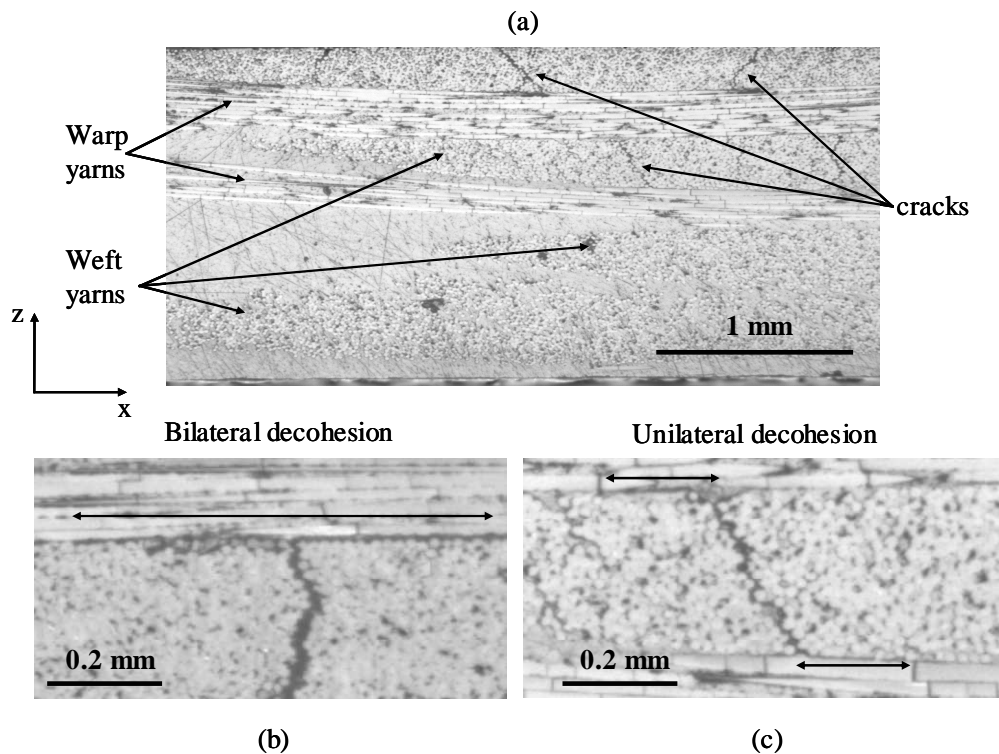


**Figure 1.** Optical microscope observations of the specimen edge with zooms on cracks of different orientations and bilateral (b) and unilateral (c) yarn-yarn decohesions at the crack tip.

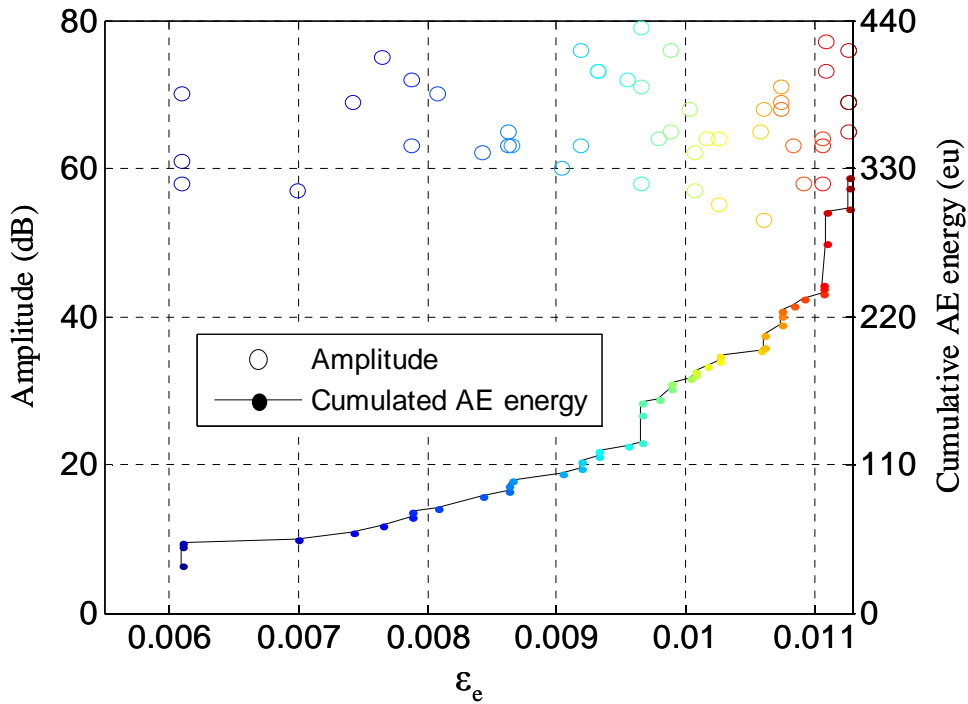


**Figure 2.** Amplitude and cumulated AE energy as a function of tensile strain.

The observed cracks extend through the whole yarn thickness in direction transverse to the fibers and at different angles with respect to the loading direction (Fig. 1a). Both bilateral (Fig. 1b) and unilateral (Fig. 1c) decohesions between yarns in contact are observed around the crack tips. The crack initiation results in a spontaneous release of elastic energy that generates waves detected by the AE sensors. The first events were observed for a global strain of  $\epsilon_{exp} = 6.10 \cdot 10^{-3}$  (Fig. 2).

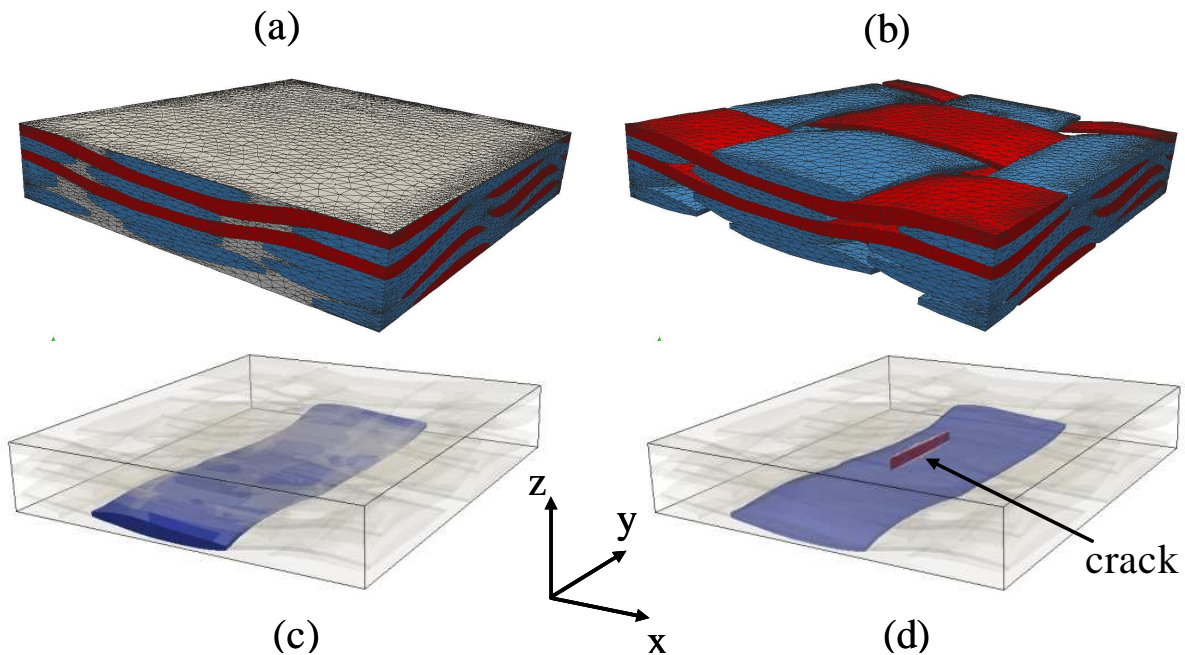


**Figure 3.** FE mesh of the composite RUC (a) and the yarns only (b). Location of the yarn under consideration in the undamaged state (c) and after insertion of a crack into the mesh (d).

Excerpt from ISBN 978-3-00-053387-7

### 3. Discrete damage modeling

The geometry of the reinforcement of a RUC is obtained by numerical modeling of the fabric compaction taking into account the multiple contacts between the yarns. The result is close to the reinforcement geometry in the real composite specimens [4]. A FE mesh of the composite RUC containing the compacted reinforcement and its matrix complement is then generated using the algorithm presented in [5]. Cracks are inserted into the mesh by first remeshing locally the undamaged mesh in order to represent the crack by the remeshed element faces [20], and then doubling the nodes at the crack surface. The FE mesh of the undamaged RUC is shown with and without matrix in Fig. 3a and b. The yarn studied in the following is highlighted in Fig. 3c without and in Fig. 3d with crack, where the element outlines are removed for the sake of clarity. The node positions and the element topology are perfectly equivalent in the undamaged and the damaged mesh, which allows to compare accurately both states in the following section.

### 4. Coupled stress and energy criterion for crack onset

The coupled criterion [15] states that two conditions must be fulfilled simultaneously to induce crack onset. The stress condition requires that the whole surface of the crack is overloaded prior to crack initiation [16], i.e.,

$$f = \left( \frac{\langle \sigma_N \rangle^+}{Y_t} \right)^2 + \left( \frac{\tau_{LT}}{S_{LT}^R (1 - p_{LT} \sigma_N)} \right)^2 + \left( \frac{\tau_{TT}}{S_{TT}^R (1 - p_{TT} \sigma_N)} \right)^2 \geq 1 \quad (1)$$

is fulfilled everywhere on the surface in the undamaged mesh, where the crack is going to be inserted. The crack criterion chosen here is based on the transverse tensile failure mode of a criterion developed for UD plies in a composite laminate [21] and transferred into the coordinates normal to the crack plane ( $N$ ), parallel to the fibers ( $L$ ) and perpendicular to the fibers in the crack plane ( $T$ ).  $Y_t$  is the transverse tensile yarn strength,  $S_{LT}^R$  and  $S_{TT}^R$  are the shear yarn strengths, and  $p_{LT}$  and  $p_{TT}$  are shape parameters that take into account the coupling between compressive stress and shear strength. The values of the different parameters are summarized in Table 1.

The energy criterion is fulfilled if the elastic energy released during crack initiation is at least equal to the energy required to create the crack surface. The former is equal to the difference between the elastic energy in the undamaged RUC  $W(0)$  and the elastic energy  $W(d)$  in the RUC with the crack inserted at the same global strain. The latter is equal to the crack surface multiplied with the critical energy release rate of the material  $G_c$ . The energy criterion can thus be written as

$$W(0) - W(d) \geq \Delta S \cdot G_c \quad (2)$$

where  $d$  is a parameter set defining the crack shape (position, length, orientation, etc.) and  $\Delta S$  the crack surface area.

For a given crack  $d$ , the strain at damage onset is determined by means of two FE calculations, one on the undamaged mesh and one on the mesh with the crack inserted. Linear elastic behavior is assumed both for the matrix and the yarns (see Table 1). The properties of the yarns are obtained from micro-

**Table 1.** Material parameters used in the FE calculations.

$E^m$	$\nu^m$	$E_L^y$	$E_T^y$	$\nu_{LT}^y$	$\nu_{TT}^y$	$G_{LT}^y$	$Y_t$	$S_{LT}^R$	$S_{TT}^R$	$p_{LT}=p_{TT}$	$G_c$
GPa		GPa	GPa			GPa	MPa	MPa	MPa	MPa <sup>-1</sup>	N/mm
3.2	0.35	41.0	9.79	0.32	0.42	7.21	35	72	45	$8.8 \cdot 10^{-3}$	0.118

meso homogenization [2], using the matrix properties given in Table 1, a Young's modulus of 73.6 GPa and a Poisson's ratio of 0.3 for the glass fibers. The stress criterion is determined on the crack surface in the undamaged mesh. Using the proportionality between the local stresses and the global strain in the composite in the case of linear elasticity, the strain at crack onset predicted by the stress criterion  $\epsilon_{stress}$  can be calculated as the lowest strain, for which the stress criterion is fulfilled over the whole crack surface. Since the energy difference in Eq. 2 is proportional to the square of the global strain, the strain at crack initiation predicted by the energy criterion  $\epsilon_{energy}$  can be determined from the difference between the elastic energies obtained with the two FE calculations as the strain, for which this energy difference reaches  $\Delta S \cdot G_c$ .

### 5. Prediction of damage onset in a woven composite

In order to limit the number of FE calculations, we first assume that the crack plane is normal to the loading direction. The influence of the crack orientation will be presented in Section 6. Since the stress criterion must be fulfilled ( $f \geq 1$ ) everywhere on the crack surface, the front of the initiated crack follows the line  $f = 1$  around a local maximum of  $f$  in the case of a crack  $d$ , for which the stress and the energy criterion are fulfilled at the same global strain ( $\epsilon_{stress}(d) = \epsilon_{energy}(d)$ ). Several FE calculations have shown that for cracks that do not extend through the whole yarn thickness, the energy criterion is fulfilled for a much larger strain than the stress criterion. We therefore consider in the following only cracks that extend through the whole yarn thickness and approximate the crack fronts by straight lines. The parameters describing such a crack are the position of its center ( $x, y$ ) and its length in yarn direction  $l$ .

Fig. 4 shows the evolution of the crack initiation strain obtained with the energy criterion as a function of the crack length  $l$  and of its position. A minimum strain of  $\epsilon_{energy}^* = 6.37 \cdot 10^{-3}$  is found for a crack of a length  $l^* = 2.02\text{mm}$  centered at  $(x^*, y^*)$ . The energy criterion thus provides a lower limit for the strain at crack onset. At a global strain of  $\epsilon_{energy}^*$ , the stress criterion is exceeded everywhere in the yarn ( $f$  between 1.1 and 1.4). Hence, in our case, the energy criterion is dominant and the crack length at initiation is given by the abscissa of the minimum of the curve shown in Fig. 4 ( $l^*$ ). The predicted strain is about 4% higher than the strain at damage onset  $\epsilon_{exp}$  detected by acoustic emission (Section 2).

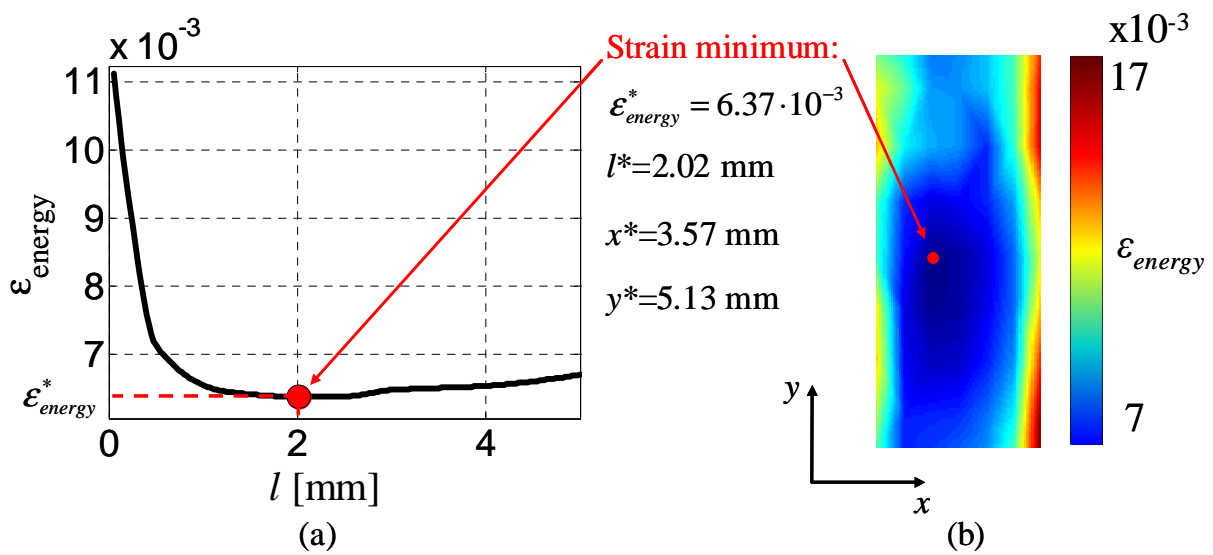


**Figure 4.** (a) Minimum of the strain at crack initiation over the yarn as a function of the crack length  $l$ , (b) strain at crack initiation as a function of the position  $(x, y)$  of the crack center for the crack length minimizing the crack initiation strain at  $(x, y)$ .

It should be noted that the crack predicted by the minimum of  $\varepsilon_{energy}^*$  is centered not exactly at, but close to the maximum of the stress criterion (at  $x^s = 3.31\text{mm}$ ,  $y^s = 6.42\text{mm}$ ). Most of the distance to the point  $(x^*, y^*)$  is in fiber direction ( $y$ ). The maximum of the stress criterion thus gives a relatively accurate estimation of the location of the crack plane, but the crack is not centered around  $(x^s, y^s)$ . The crack initiation strain obtained by minimizing  $\varepsilon_{energy}$  as a function of the crack length for cracks located at  $(x^s, y^s)$  is  $6.8 \cdot 10^{-3}$ ; which is about 7% higher than  $\varepsilon_{energy}^*$  and 11% higher than  $\varepsilon_{exp}$ . The corresponding crack length is 3.4mm, which is significantly longer than the length of the crack minimizing  $\varepsilon_{energy}$  over the whole yarn.

The maximum of the stress criterion reaches 1 at a global strain of  $2.7 \cdot 10^{-3}$ . However, due to the localized character of the stress concentration at this maximum (even if there is no singularity), this value depends on the FE mesh. Therefore, regularization methods based on a non-local measure of stress (the average stress over a zone around the maximum or the stress at a given distance from the maximum) are often used to determine damage onset at stress concentrations. In the presented case, the stress criterion exceeds 1 over the whole surface of a small semi-elliptical crack (half axes 0.07mm and 0.5mm) centered at  $(x^s, y^s)$  at a global strain of  $2.9 \cdot 10^{-3}$ . The energy released by the initiation of this crack would reach  $\Delta S \cdot G_c$  only for a much higher strain of  $17.7 \cdot 10^{-3}$ . Since both conditions are necessary, such a small crack cannot initiate at the strain predicted by the stress criterion. Thus, the stress criterion alone, whether delocalizing regularization methods are used or not, significantly underpredicts strain at damage onset. Without regularization, this prediction will in addition depend on the FE mesh, whereas the difference between the elastic energy of the undamaged and the cracked RUC is almost mesh independent, because the difference is calculated between two identical meshes with the same node positions and element topologies, except for the duplication of the nodes at the crack surface.

## 6. Crack orientation and decohesions around the crack tip

The energy difference (Eq. 2) has been calculated for different crack orientations, in order to determine whether a crack plane normal oriented at an angle  $\theta \neq 0^\circ$  from the loading direction leads to higher energy releases and thus the initiation of such a crack occurs at a lower strain. For the crack minimizing the energy criterion (located at  $(x^*, y^*)$  and of length  $l^*$ ), the minimum crack initiation strain is indeed obtained for a crack normal to the loading direction ( $\theta = 0^\circ$ ). The same study has been repeated for different crack lengths (Fig. 5a) and for different crack center locations, leading to the conclusion that at least within a limited zone around  $(x^*, y^*)$  the optimum crack orientation is independent of the crack position and length and can thus be optimized separately. This greatly reduces the number of FE calculations necessary to determine the crack configuration at damage onset. It should also be noted that the crack orientation may well be different from  $\theta = 0^\circ$ , if a different RUC or a different yarn (for the initiation of the 2<sup>nd</sup> or 3<sup>rd</sup> crack, for example) is studied.

Experimental observations (Section 2) show that transverse yarn cracks are usually accompanied by yarn-yarn decohesions around the crack tips. Therefore, different crack configurations, with and without unilateral or bilateral decohesions were analyzed in terms of the stress and the energy criterion. Whereas the stress criterion is not fulfilled on the yarn-yarn interface, the energy criterion yields a smaller initiation strain for small decohesion lengths (up to  $\mu^* = 0.09\text{mm}$ ) than without decohesions (Fig. 5b). This means that at damage onset, no decohesions will be generated, because of the stress criterion, but as soon as the yarn has cracked, a stress singularity emerges at the crack tip. Therefore the stress criterion is exceeded locally around the crack tip, allowing decohesions to propagate. Since at the initiation of the transverse yarn crack, the global strain is already higher than energetically necessary to open the crack together with the decohesion (equality of Eq. 2 for the total surface of crack and decohesion), the decohesion will propagate instantaneously up to the length  $\mu^*$ , at which the equality of Eq. 2 is fulfilled for the strain at crack initiation  $\varepsilon_{energy}^*$ .

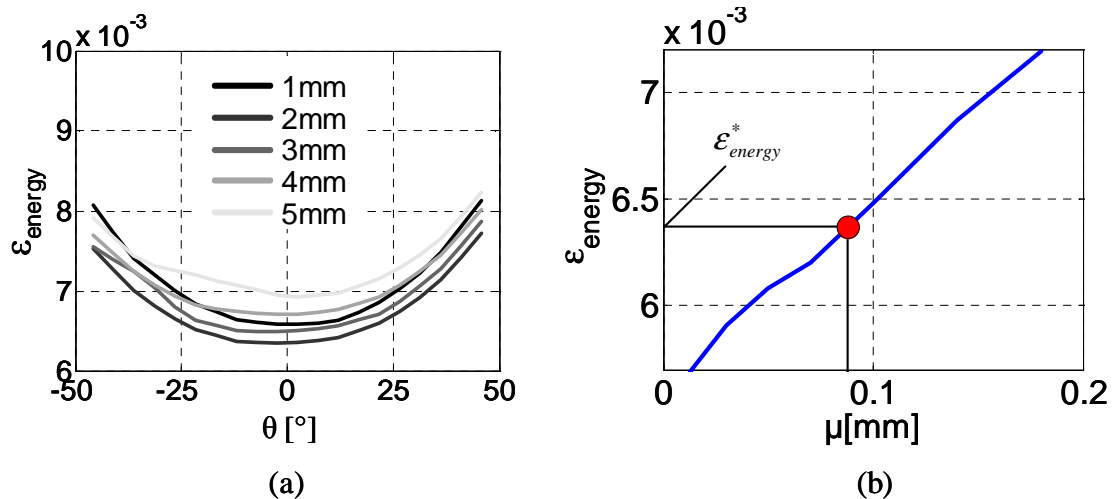


**Figure 5.** Damage onset strain obtained with the energy criterion for a crack centered at  $(x^*, y^*)$  as a function of the crack orientation for different crack lengths (a), and as a function of the decohesion length for a crack of length  $l^*$  and  $\theta = 0^\circ$  (b).

## 7. Conclusions

Prediction of crack initiation in textile composites with a stress based criterion can lead to a significant underestimation of the strain at damage onset if energy aspects are neglected, and even if delocalized criteria such as the average stress or the point stress method are used. Comparing the energy released by the crack initiation to the energy required to generate its surface yields an estimate closer to experimental observations by acoustic emission. With this energy criterion, the crack configuration (location, length, orientation, and decohesion configuration and length) can be determined. The number of calculations required to determine the crack initiation configuration grows, in theory, exponentially with the number of parameters describing the crack. However, some parameters are uncoupled, which reduces the computational costs. In the presented work, the coupled criterion has been used to predict the first crack initiation. In the future, the criterion will successively be applied on cracked RUCs to determine the cracking sequence and damage kinetics in textile composites, as well as to study the influence of the material parameters on damage onset and evolution.

## References

- [1] M. Zako, Y. Uetsuji, and T. Kurashiki. Finite element analysis of damaged woven fabric composite materials. *Composites Science and Technology*, 63:507-516, 2003.
- [2] P. Melro, P. Camanho, F.M. Andrade Pires, and S.T. Pinho. Numerical simulation of the non-linear deformation of 5-harness satin weaves. *Computational Materials Science*, 61:116-126, 2012.
- [3] D.S. Ivanov, S.G. Ivanov, S.V. Lomov, and I. Verpoest. Unit cell modelling of textile laminates with arbitrary inter-ply shifts. *Composites Science and Technology*, 72:14-20, 2011.
- [4] A. Doitrand, C. Fagiano, F.-H. Leroy, A. Mavel, and M. Hirsekorn. On the influence of fabric layer shifts on the strain distributions in a multi-layer woven composite. *Composite Structures*, 145:15-25, 2016.
- [5] G. Grail, M. Hirsekorn, A. Wendling, G. Hivet, and R. Hambli. Consistent Finite Element mesh generation for meso-scale modeling of textile composites with preformed and compacted reinforcements. *Composites Part A*, 55:143-151, 2013.
- [6] A. Doitrand, C. Fagiano, V. Chiaruttini, F.-H. Leroy, A. Mavel, and M. Hirsekorn. Experimental characterization and numerical modeling of damage at the mesoscopic scale of woven polymer

- matrix composites under quasi-static tensile loading. *Composites Science and Technology*, 119:1-11, 2015.
- [7] S. Daggumati, W. Van Paepegem, J. Degrieck, J. Xu, S.V. Lomov, and I. Verpoest. Local damage in a 5-harness satin weave composite under static tension: Part II Meso-FE modelling. *Composites Science and Technology*, 70:1934-1941, 2010.
- [8] S.V. Lomov, D.S. Ivanov, I. Verpoest, M. Zako, T. Kurashiki, H. Nakai, and S. Hirosawa. Meso-FE modelling of textile composites: Road map, data flow and algorithms. *Composites Science and Technology*, 67:1870-1891, 2007.
- [9] J.C. Faes, A. Rezaei, W. Van Paepegem, and J. Degrieck. Accuracy of 2D FE models for prediction of crack initiation in nested textile composites with inhomogeneous intra-yarn fiber volume fractions. *Composite Structures*, 140:11-20, 2016.
- [10] L. Gorbatikh, D.S. Ivanov, S.V. Lomov, and I. Verpoest. On modelling of damage evolution in textile composites on meso-level via property degradation approach. *Composites Part A*, 38:2433-2442, 2007.
- [11] O. Allix, P. Feissel, and P. Thevenet. A delay damage mesomodel of laminates under dynamic loading: Basic aspects and identification issues. *Computers & Structures*, 81:1177-1191, 2003.
- [12] P. Maimí, P.P. Camanho, J.A. Mayugo, and C.G. Davila. A continuum damage model for composite laminates: Part II Computational implementation and validation. *Mechanics of Materials*, 39:909-919, 2007.
- [13] B.H. Le Page, F.J. Guild, S.L. Ogin, and P.A. Smith. Finite element simulation of woven fabric composites. *Composites Part A*, 35:861-872, 2004.
- [14] E. Obert, F. Daghia, P. Ladevèze, and L. Ballere. Micro and meso modeling of woven composites: Transverse cracking kinetics and homogenization. *Composite Structures*, 117:212-221, 2014.
- [15] D. Leguillon. Strength or toughness? A criterion for crack onset at a notch. *European Journal of Mechanics A/Solids*, 21:61-72 (2002).
- [16] P. Weißgraber, D. Leguillon, and W. Becker. A review of finite fracture mechanics: Crack initiation at singular and non-singular stress raisers. *Archive of Applied Mechanics*, 86:375-401, 2016.
- [17] E. Martin, D. Leguillon, and N. Carrère. A coupled strength and toughness criterion for the prediction of the open hole tensile strength of a composite plate. *International Journal of Solids and Structures*, 49:3915-3922, 2012.
- [18] E. Martin, D. Leguillon, and N. Carrère. A twofold strength and toughness criterion for the onset of free-edge shear delamination in angle-ply laminates. *International Journal of Solids and Structures*, 47:1297-1305, 2010.
- [19] V. Mantič and I.G. Garcia. Crack onset and growth at the fibre-matrix interface under a remote biaxial transverse load. Application of a coupled stress and energy criterion. *International Journal of Solids and Structures*, 49:2273-2290, 2012.
- [20] V. Chiaruttini, V. Riolo, and F. Feyel. Advanced remeshing techniques for complex 3D crack propagation. *Proceedings of the 13<sup>th</sup> International Conference on Fracture ICF13, Beijing, China, July 16-21 2013*, pp. 547-555.
- [21] J.S. Charrier, N. Carrère, F. Laurin, T. Bretheau, E. Goncalves-Novo, and S. Mahdi. Proposition of a 3D progressive failure approach and validation on test cases. *Proceedings of the 14<sup>th</sup> European Conference of Composite Materials ECCM14, Budapest, Hungary, June 7-10 2010*.